Ordering and bandgap reduction in $InAs_{1-x}Sb_x$ alloys†

D M Follstaedt, R M Biefeld, S R Kurtz, L R Dawson and K C Baucom

Sandia National Laboratories, Albuquerque, NM 87185-1056 USA

Abstract. $InAs_{1-x}Sb_x$ alloys grown by MBE and MOCVD are found to have reduced emission energies due to CuPt-type order, even for Sb concentrations as low as x = 0.07 (ΔE = 25-65 meV). Cross-section TEM examination of such alloys shows the two $\{111\}_B$ variants are separated into regions 1-2 μm across with platelet domains 10-40 nm thick on habit planes tilted ~30° from the (001) growth surface. Nomarski optical images show a cross-hatched surface pattern expected for lattice-mismatched layers. The local tilt of the surface correlates with the dominant variant in each region. $InAs_{1-x}Sb_x$ /$In_{1-y}Ga_yAs$ strained-layer superlattices with low Sb content and flat surfaces also show CuPt ordering.

This work was supported by the United States Department of Energy under Contract DE-AC04-94AL85000.

1. Introduction

Alloys of $InAs_{1-x}Sb_x$ have the lowest bandgaps of ternary III-V alloys and are of interest for potential use as infrared detectors and emitters. We have used molecular beam epitaxy (MBE) and metallorganic chemical vapor deposition (MOCVD) to grow layers of this alloy as well as strained-layer superlattices (SLS) with it as a constituent. The optical emission energies of our materials [1] are systematically below the bandgaps of bulk alloys [2]. We have examined the alloys with cross-section transmission electron microscopy (XTEM) and found that all contain CuPt-type order [3-5], which is expected to reduce bandgaps in this alloy system [6]. Ordering is found even for Sb concentrations as low as x = 0.07. Here we discuss order in mid-concentration alloys (x ≈ 0.4) of potential use as long-wavelength infrared detectors and then examine order in low-Sb alloys (x = 0.07-0.14) for mid-wavelength emitters and detectors. The latter are being used in SLSs of $InAs_{1-x}Sb_x$ /$In_{1-y}Ga_yAs$ for lasers [7], and these $InAs_{1-x}Sb_x$ layers also contain CuPt order.

Another non-random alloy structure, phase separation into two compositions, could also give reduced emission energies. Phase separation occurs on a coarse scale (30-50 nm) in $InAs_{1-x}Sb_x$ alloys grown below 400°C and even occurs with CuPt ordering [8-10]. Our alloys are grown above this temperature and the coarse separation is avoided. The x = 0.07 alloy does not show evidence of either coarse- or fine-scale (~10 nm) phase separation [5], and we therefore attribute its reduced emission energy to CuPt order. Preparation of thin XTEM specimens of these fragile alloys is discussed elsewhere [5].

We previously investigated an alloy grown by MBE at 425°C with x = 0.4 and found CuPt-type ordering reflections at ½{111} and related positions [3]. Ordering was also found by Seong et al. [8] for MBE alloys with x = 0.2 - 0.8, but was strongest near 0.5, as expected from the ideal CuPt stoichiometry. Their specimens were grown at 370°C, for which phase

DISCLAIMER

separation occurred. Recent evaluations by Seong et al. [10] of their alloys with x = 0.5 indicate that growth temperatures of 370-400°C give maximum ordering, and also that it occurs in the As-rich phase, $InAs_{0.74}Sb_{0.26}$; however, they did not detect order at 450°C and above. Our alloys are thus expected to have a reduced degree of order due to higher growth temperatures (425-525°C), but ordering in As-rich alloys is not unexpected.

The optical emission energy of our $InAs_{0.60}Sb_{0.40}$ alloy was 132 meV (λ = 9.4 μm), while that expected for bulk alloys is 177 meV [2]. A SLS with a similar alloy and a type-II offset from adjacent layers gave an emission energy of 117 meV, and the photoconductive response was found to extend to 10.6 μm, or ~80 meV lower than for bulk bandgaps. The photoresponse of a phase-separated "natural superlattice" grown at 340°C extended to 12.5 μm [11]. These results indicate that ordered $InAs_{1-x}Sb_x$ alloys can have bandgaps low enough to span the 8-12 μm atmospheric window for detection.

2. Low-Sb Concentration Alloys

We detected CuPt order in [110] electron diffraction patterns from MOCVD alloys with x = 0.07 and 0.14 grown at 475°C on InAs substrates. In addition, the relative intensities of the two variants changed with location; regions 1 - 2 μm across could be found in which one variant was dominant or existed alone. Here we examine the domain structure of these regions in the x = 0.14 alloy.

The top of the alloy layer (1.7μm total thickness) is shown in the bright-field XTEM image in Fig. 1a. Near the center and right-hand side of the image, dark linear features are seen, which tilt downward to the left. The diffraction pattern in Fig. 1b was taken from this region, and indicates that one variant dominates. On the left side of Fig. 1a, similar linear features are seen which tilt in the opposite direction; diffraction from this region (not shown) indicates that the other variant dominates. The approximate boundary between the two regions in indicated with a dashed line extending to the surface. The surface is not flat; many areas show peaks and valleys. The peaks are 20-60 nm above the valleys, with surface tilts of 2 - 4°. Note that the direction of surface tilt in Fig. 1a above the center and right is toward the $<111>_B$ direction of the dominant variant in Fig. 1b, while the opposite tilt occurs on the left-hand side with the other variant. In several alloys, such tilting by a few degrees has been shown to favor the corresponding variant [11-13].

The surface roughness is quite evident in Nomarski optical micrographs, as seen in Fig. 3. This figure shows a cross-hatched pattern on the surface like that expected for lattice-mismatched layer/substrate combinations. Two sets of orthogonal lines are seen along the [100] and [010] directions. The "sense" of the illumination in this image is that of light coming from the upper left corner, and lines at 45° to [100] are also seen.

X-ray diffraction was used to determine the lattice constants of the layer and thereby determine its composition and degree of lattice relaxation. By using two reflections, one with a reciprocal lattice vector normal to the surface and one having an in-plane component, the lattice constants of the layer in the orthogonal and parallel directions can be obtained. This determines the composition accurately even when lattice relaxation is incomplete. For this alloy, $a_\perp$ = 0.61324 nm and $a_\parallel$ = 0.61058 nm, giving a relaxed lattice constant of a_0 = 0.61186 nm, which corresponds to x = 0.14 and 1.0% lattice mismatch with the InAs substrate (0.60585 nm). The $a_\parallel$ value is positioned 79% of way from the substrate a_0 to the unstrained a_0, indicating that significant relaxation has occurred, which is consistent with the Nomarski image. The layer/substrate interface shows a high density of misfit dislocations [5], and defects pass through the layer to the surface as seen in Fig. 1a.

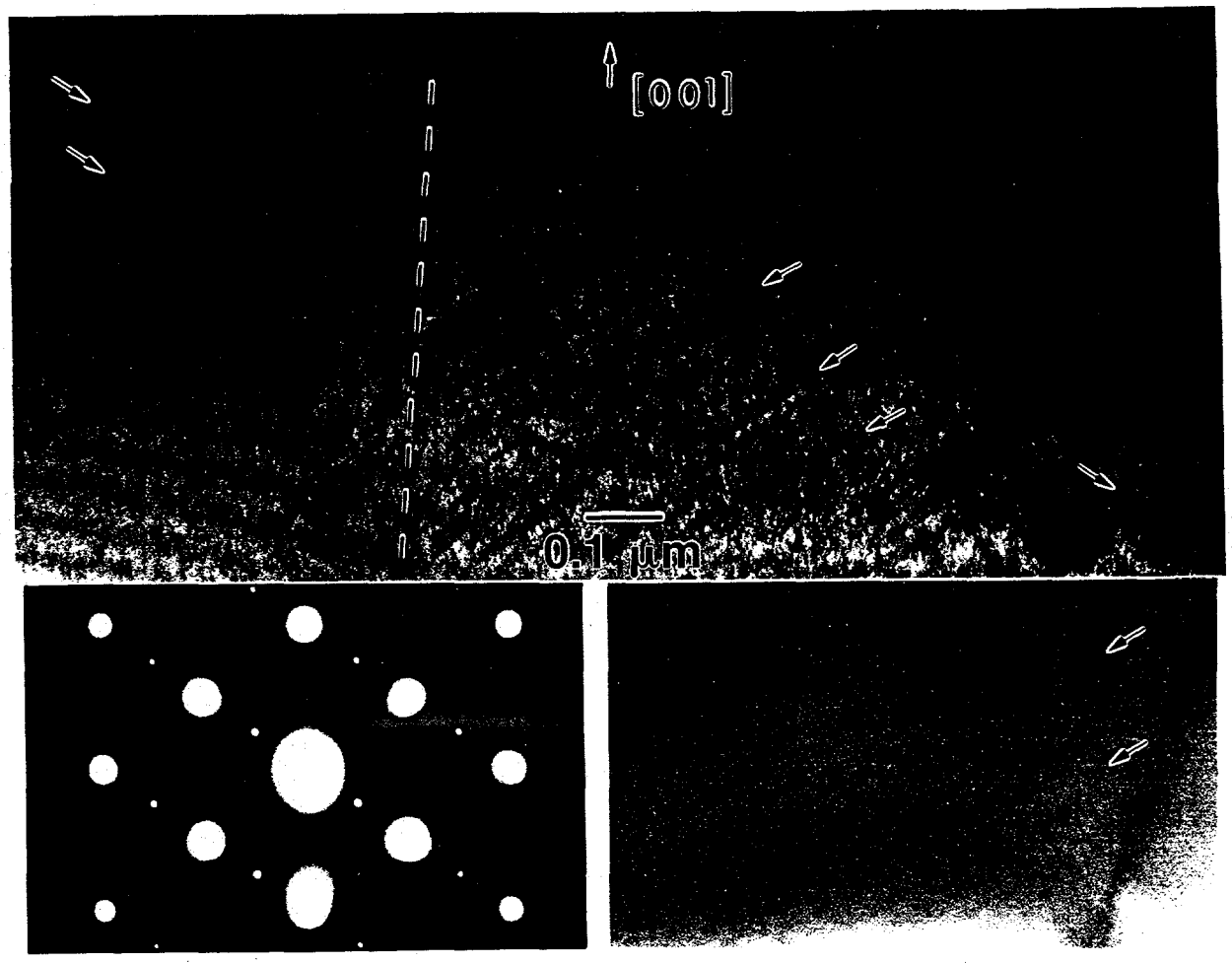

Figure 1. a) Bright-field XTEM image of $InAs_{0.86}Sb_{0.14}$ alloy grown by MOCVD on InAs at 475°C. Dashed line divides two regions with different variants (arrows). b) Diffraction pattern from region to the right of center in a). c) Dark-field image of ordered domains in the lower right side of a).

Considering strain relaxation, surface tilting, and correlation of variant with tilt, the formation of an alloy layer with regions alternating between the two $\{111\}_B$ variants is seen to be closely related to lattice mismatch of the alloy and substrate. Surface tilting results from misfit dislocations and selects one variant locally during growth. The 2 - 4° tilts are mainly due to atomic surface steps, since the angular width of the (004) x-ray reflection shows misorientations of the atomic planes by only ~0.5°. A similar separation of variants due to surface tilts has been seen in (In,Ga)P, but the tilting has a different origin [13].

The direct identification of the linear contrast in Fig. 1a with order requires dark-field imaging of the domains with the ½{111}-type reflections. These reflections are weaker than those of alloys with x = 0.4 [3] and those of $In_{0.5}Ga_{0.5}P$ [14], but we are barely able to obtain images with the domains illuminated. Figure 1c is such an image (contrast enhanced) from the lower right-hand side of Fig. 1a, with illuminated linear features similar to the dark ones in Fig. 1a. We thus conclude that the dark linear features in bright-field are the ordered domains. They appear to be platelets viewed edge-on and are 10 - 40 nm thick. They lie on habit planes tilted ~30° from (001) in the same direction as the surface tilt.

Order is incomplete in the $InAs_{0.86}Sb_{0.14}$ alloy, as expected from the ideal (1:1) CuPt stoichiometry. The separated platelets in Figs. 1a and 1c indicate that ordered domains are in a disordered matrix. Also, high-resolution images (not shown) have ordering contrast that starts and stops along $\{111\}_B$ planes, implying that order is not continuous within domains.

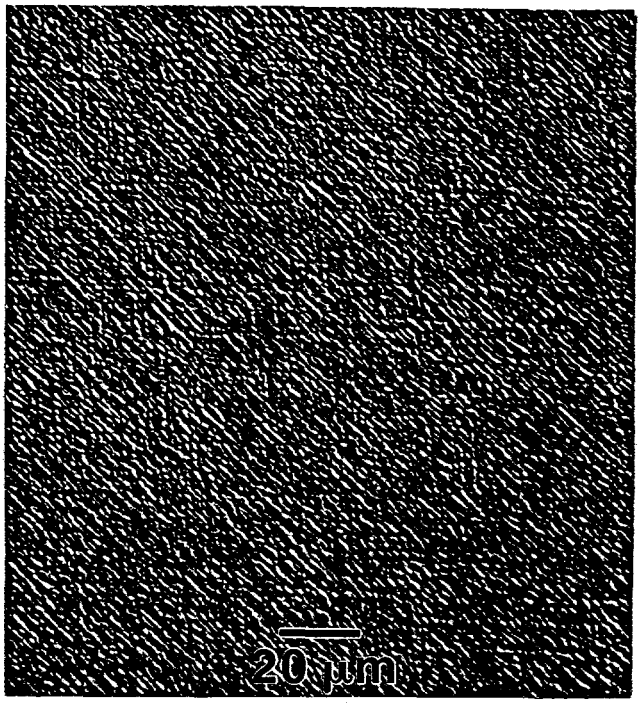

Figure 2. Nomarski image of $InAs_{0.86}Sb_{0.14}$ alloy surface grown by MOCVD at 475°C on InAs. Linear features are valleys and crests. (CVD1088).

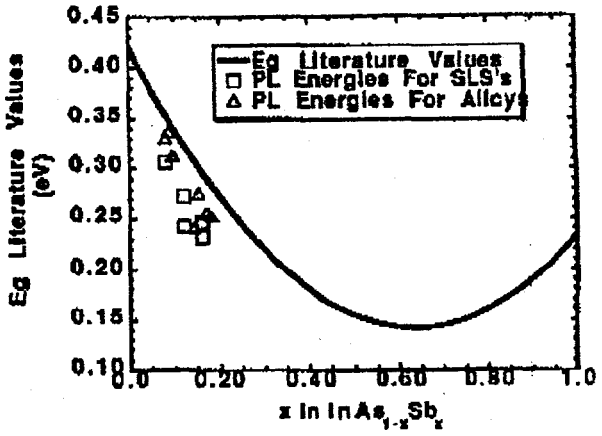

Figure 3. $InAs_{1-x}Sb_x$ bandgap vs. x. Solid line- bulk and OMVPE from [2]. Symbols - our MOCVD results.

In Fig. 3, emission energies of our low-Sb alloys and SLSs are plotted versus Sb concentration along with a curve from Fang et al. [2] representing their OMVPE data and bulk alloy data. Our data systematically fall below the curve, evidently due to CuPt ordering. The difference from their vapor-grown alloys is not understood. It could be related to measurement of composition or to growth parameters. However the only notable difference in growth is rate (our 1.7 μm/hr vs. 0.5 μm/hr) and it does not appear substantial.

3. Low-Sb Concentration Strained-Layer Superlattices

We are investigating SLSs of $InAs_{1-x}Sb_x/In_{1-y}Ga_yAs$ to form improved mid-wavelength infrared emitters. By correctly choosing concentrations, such as x = 0.09 and y = 0.13 to be discussed here, the average in-plane lattice constant can be matched to InAs. The SLS also provides an in-plane strain to the $InAs_{1-x}Sb_x$ layer that reduces non-radiative Auger transitions of excited carriers [7]. The increased optical efficiency may allow lasing to be achieved at higher temperatures. However, the emission energy is still below the bandgap of bulk $InAs_{1-x}Sb_x$ alloys, as seen in Fig. 3. Figure 4a shows an electron diffraction pattern from the SLS. Very weak CuPt ordering reflections of both variants are seen, along with wavy streaks along the [001] direction. The microstructure of this order is seen in Fig. 4b to be small regions of one variant as detected by the doubled periodicity (light/dark variations) in the high-resolution lattice image along the arrowed $\{111\}_B$ planes. These two regions are in 10 nm-thick $InAs_{1-x}Sb_x$ layers of the SLS [15]. The SLS layers are flat with no tilt preference for either variant, but small single-variant regions 10-20 nm wide nonetheless form during growth at 475°C. Other alloys and SLSs grown at up to 525°C also emit at energies below bulk bandgaps, implying that order is not eliminated at this temperature.

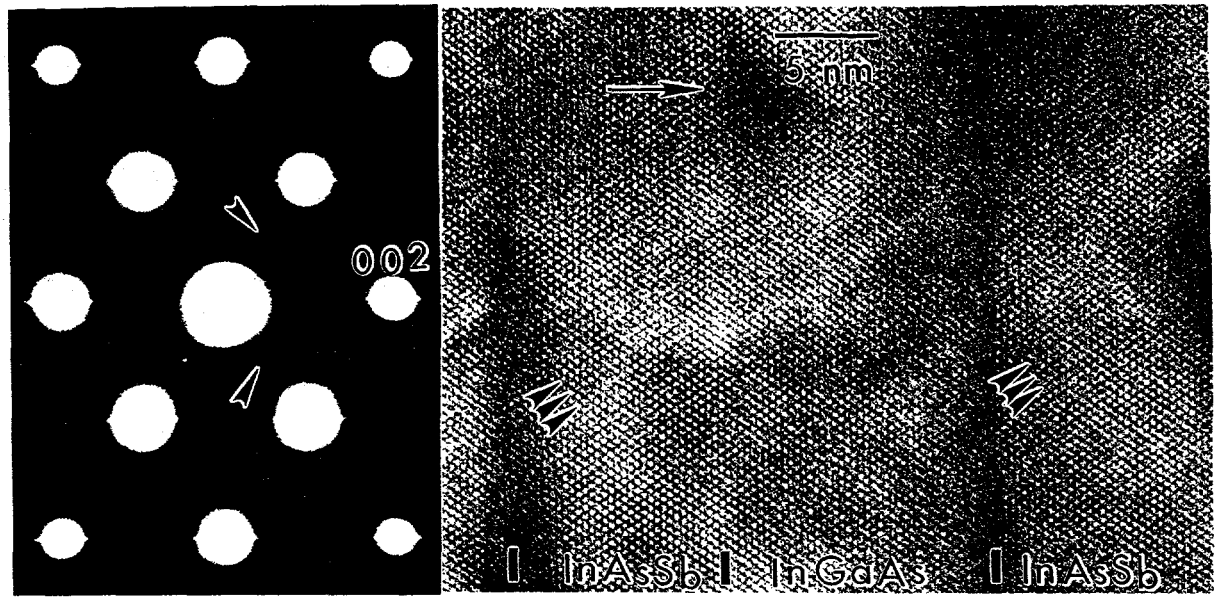

Figure 4. a) [110] diffraction pattern from $InAs_{0.81}Sb_{0.09}/In_{0.87}Ga_{0.13}As$ SLS with CuPt reflections marked. b) High-resolution lattice image with order (alternating dark/light) along $\{111\}_B$ atomic planes (arrowed). Growth direction is shown with large arrow. (Specimen CVD 1172).

References

† This work was supported by the United States Department of Energy under Contract DE-AC04-94AL85000.

[1] Biefeld R M, Baucom K C and Kurtz S R 1994 J. Crystal Growth **137** 231-234.

[2] Fang Z M, Ma K Y, Jaw D H, Cohen R M and Stringfellow G B 1990 J. Appl. Phys. **67** 7034-7039.

[3] Kurtz S R, Dawson L R, Biefeld R M, Follstaedt D M and Doyle B L 1992 Phys. Rev. **B46** 1909-1912.

[4] Biefeld R M, Baucom K C, Kurtz S R and Follstaedt D M 1994 Mat. Res. Soc. Symp. Proc. **325** 493-498.

[5] Follstaedt D M, Biefeld R M, Kurtz S R and Baucom K C 1995 , submitted to Journal of Electronic Materials.

[6] Wei S-H and Zunger A 1991 Appl. Phys. Lett. **58** 2684-2686.

[7] Kurtz S R, Biefeld R M, Dawson L R, Baucom K C and Howard A J 1994 Appl. Phys. Lett. **64** 812-814.

[8] Seong T-Y, Norman A G, Booker G R, Droopad R, Williams R L, Parker S D, Wang P D and Stradling R A 1990 Mat. Res. Soc. Symp. Proc. **163** 907-912.

[9] Seong T-Y, Norman A G, Ferguson I T and Booker G R 1993 J. Appl. Phys. **73** 8227-8236.

[10] Seong T-Y, Booker G R, Norman A G and Ferguson I T 1994 Appl. Phys. Lett. **64** 3593-3595.

[11] Chen G S and Stringfellow G B 1991 Appl. Phys. Lett. **59** 3258-3260.

[12] Su L C, Ho I H and Stringfellow G B 1994 J. Appl. Phys. **75** 5135-5141.

[13] Friedman D J, Zhu J G, Kibbler A E and Olson J M 1993 J. Appl. Phys. **63** 1774-1776.

[14] Follstaedt D M, Schneider R P, Jr and Jones E D 1995, submitted to Journal of Applied Physics

[15] Biefeld R M, Follstaedt D M, Kurtz S R and Baucom K C 1995 , elsewhere these proceedings. This paper discusses the SLS structure in more detail.